Article

Synthesis and Structure-Activity Relationship of a WO₃ Catalyst for the Total Oxidation of BTX

Rosana Balzer,[*,a] *Valderez Drago,*[b] *Wido H. Schreiner*[c] *and Luiz F. D. Probst*[a]

[a]*Department of Chemistry and* [b]*Department of Physics, Federal University of Santa Catarina (UFSC), 88040-900 Florianópolis-SC, Brazil*

[c]*Department of Physics, Federal University of Paraná (UFPR), 81531-970 Curitiba-PR, Brazil*

Neste estudo foi preparado um catalisador à base de WO₃ para investigar a atividade catalítica na oxidação total de compostos orgânicos voláteis conhecidos como benzeno, tolueno e xileno (BTX). Para uma faixa de temperaturas baixas (50-450 °C) os únicos produtos de reação foram CO₂ e H₂O. Os resultados de caracterização para o catalisador sugerem que a elevada atividade catalítica pode ser atribuída aos efeitos de interação forte do metal, o que é possivelmente originada a partir da pequena diferença entre o parâmetro de rede e os planos (111), (020) e (002), assim como a presença de espécies W⁴⁺, W⁵⁺ e W⁶⁺ sobre a superfície do catalisador, que reagem com espécies de oxig**ê**nio ativo.

In this study we prepared a WO₃-based catalyst to investigate its catalytic activity in the total oxidation of the volatile organic compounds known as benzene, toluene and xylene (BTX). For a range of low temperatures (50-450°C) the only reaction products were CO₂ and H₂O. The results for the catalyst characterization suggested that the high catalytic activity could be attributed to the effects of a strong metal interaction, which is possibly originated from the small lattice parameter difference between the (111), (020) and (002) lattice planes and the presence of W⁴⁺, W⁵⁺ and W⁶⁺ species on the surface of the catalyst which react with active oxygen species.

Keywords: tungsten oxide, catalytic oxidation, BTX

Introduction

Volatile organic compounds (benzene, toluene and xylenes, BTX) present in air are derived from various industrial processes and they are harmful to human health and to the environment even at low concentrations.[1,2] It is widely recognized that the emission of BTX compounds is a critical environmental problem and thus several techniques for the reduction of these compounds have been investigated. The catalytic oxidation of BTX to control gaseous industrial emissions is one of the most promising environmental technologies.[3] Catalytic oxidation is one of the most important methods for the removal of BTX from air.[1] Many environmental problems, such as toxicity and petrochemical smog are related to BTX emissions.[4] Catalytic oxidation does not require the addition of fuel, which reduces energy consumption and avoids the formation of thermal NOx.[4,5] This process is regarded as

*e-mail: rosanabalzer@gmail.com

effective because it operates at low temperatures and there is no formation of byproducts from thermal oxidation.[4] The design of the catalytic system and the development of selective catalysts of low cost are crucial points for the success of the process. Typical catalysts for BTX oxidation such as platinum (Pt) and gold (Au) are typically used to promote these reactions. However, due to the high cost of these metals, they are increasingly being replaced with cheaper catalysts based on transition metals, such as tungsten oxide. Metal oxides have attracted much interest in various areas of research, including studies on catalytic oxidation, and it has been reported that tungsten oxides have excellent catalytic activity.[6-8] Feng *et al*.[9] synthesized a tungsten-based catalyst, which shows good activity (80% conversion) in studies on the epoxidation of cyclooctene.[9-11] The reports in the literature on the different catalysts which are active in the oxidation of BTX were reviewed and the transition metal oxide complex V₂O₅-WO₃/TiO₂ appears to be suitable for this application and different reactor geometries have also been described, however, they

are expensive.[12] Tungsten oxide is a solid with an acidic character which has many applications in heterogeneous catalysis and it has the ability to form a large variety of stoichiometric and nonstoichiometric oxides depending on the atmosphere and thermal treatment applied being a promising candidate for catalytic oxidation reactions.[13,14]

Therefore, there is a clear need to develop cheaper active and selective catalysts by improving either the support or the active phase. In this study, we investigated the catalytic behavior of a WO_3 catalyst, particularly in relation to the complete catalytic oxidation of benzene, toluene and xylene.

Experimental

Catalyst preparation and characterization

A suspension of 2 g of tungsten in 10 mL of 50% hydrogen peroxide was prepared and kept at 50 °C until evaporation of 50% of the peroxide volume. Next, 2.0 mL of a H_3PO_4 solution (40%) and 10 mL of distilled water were added and the solvent was evaporated in a rotary evaporator inside a thermostated bath at 70 °C. Subsequently, the sample was dried in an oven for 24 h at 100 °C and then calcined in a muffle furnace with circulating air at a heating rate of 5 °C min^{-1} starting at ambient temperature and increasing to 750 °C, this temperature being held for 4 h.

Infrared spectra were obtained from 400 to 1400 cm^{-1} for which the samples (2 mg) were mechanically blended with 200 mg of KBr. The data were recorded using a Fourier transform (FT) Perkin-Elmer 16 PC infrared spectrophotometer. The morphology and microstructure of the catalyst were observed by scanning electron microscopy (SEM, JEOL JSM-6390LV) and field emission transmission electron microscopy (FETEM, JEOL JEM-1011). The chemical composition and metal content of the catalyst were analyzed by energy-dispersive X-ray spectroscopy (EDX). The specific surface area of the catalyst (S_{BET}) was determined using a Nova 2200e analyzer (Quantachrome Instruments). The surface areas were calculated applying the Brunauer-Emmett-Teller (BET) method employing isothermal gas adsorption/desorption of N_2 at 77 K considering 40 points. The crystalline structure of the catalyst was analyzed by X-ray powder diffraction (XRD, Bruker-AXS Siemens) with CuKα radiation (V = 40 kV; I = 30 mA). The binding energies of the elements were determined by X-ray photoemission spectroscopy (XPS, VG Microtech 3000). The O_2-chemisorption measurements were conducted at 600 °C using a ChemBET analyzer (Quantachrome Instruments).

Catalytic activity tests

Catalytic activity tests were carried out at atmospheric pressure in a fixed-bed quartz tubular reactor, with 9 mm of inner diameter, packed with 10 mg of catalyst, and the temperature range was 50-350 °**C.** The heating furnace had dimensions of 30 cm diameter and 60 cm length. The following conditions were chosen: inlet benzene (Vetec®) concentration 2.0 g m^{-3}, toluene (Vetec®) concentration 1.5 g m^{-3} and *m/p*-xylene (Vetec®) concentration 1.0 g m^{-3} in air. Air was used as the carrier gas at a total flow rate of 20 mL min^{-1}. The kinetics data were collected after at least 1 h on-stream at room temperature. The only products were CO_2 and H_2O as determined on a gas chromatograph (GC, Varian 3400), equipped with a thermal conductivity detector (TCD) and a flame ionization detector (FID) connected in series. The chromatography columns used were of the HP-Plot-Q and HP-5 types, both with a length of 30 m and diameter of 0.53 mm.

The catalytic activity was expressed as the degree of conversion of the BTX calculated as follows: *BTXs (%)* = percentage of BTXs converted; $[BTXs]_{in}$ = input BTX concentration; $[BTXs]_{out}$ = output BTX concentration. Turnover frequency (TOF, h^{-1}) was 415 h^{-1}.

$$BTXs\,(\%) = \frac{[BTXs]_{in} - [BTXs]_{out}}{[BTXs]_{in}} \times 100\% \qquad (1)$$

Results and Discussion

Catalyst characterization

The infrared spectrum shown in Figure 1 clearly shows vibrations at 425, 430, 725, 865, 930 and 970 cm^{-1}, which are characteristic of tungsten oxide. The peaks at 970, 725, 425 and 430 cm^{-1} are assigned to the monoclinic phase WO_3. The vibrational band at 948 cm^{-1} is also a typical WO_3 phase.[15] The band at 865 cm^{-1} is attributed to W–O stretching, which characterizes the presence of monoclinic WO_3. An acute and intense band at around 910 cm^{-1} can also be observed, which is attributed to W=O stretching. The spectrum also shows an intense broad band located in around 960 cm^{-1}, due to W–O–W stretching. The band at approximately 922 cm^{-1} can be attributed to W–O vibrations with respect to oxygen atoms in the bridge and terminal WO_3.[1,15,16]

The values for the surface area, pore volume and pore diameter of the catalyst are given in Table 1. The isotherms (Figure 2) obtained revealed that the catalysts have pores of regular cylindrical and/or polyhedral shape. They are type IV isotherms, a finding which is typical of mesoporous materials. Hysteresis type H1 was observed at high relative
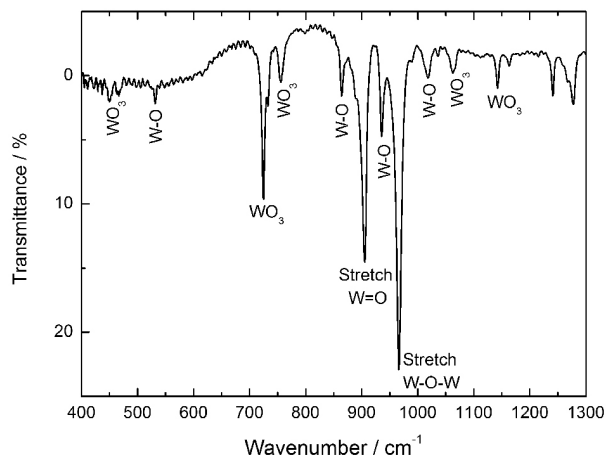
Figure 1. Infrared spectrum for WO$_3$ catalyst.

pressures and this can be attributed to the formation of textural mesoporosity.

The X-ray diffractograms are shown in Figure 3. The diffraction peaks ($2\theta = 16, 23, 26, 29, 34, 35, 38, 49, 52, 56$ and $62°$) are assigned to the reflections associated with the tungsten oxide (WO$_3$) phase, a monoclinic crystal system (JCPDS data file 01-072-1465). The peak at $2\theta = 23°$ is characteristic of tungsten oxide (WO$_{2.95}$). The peaks are more intense for WO$_3$ (111) ($2\theta = 26°$).
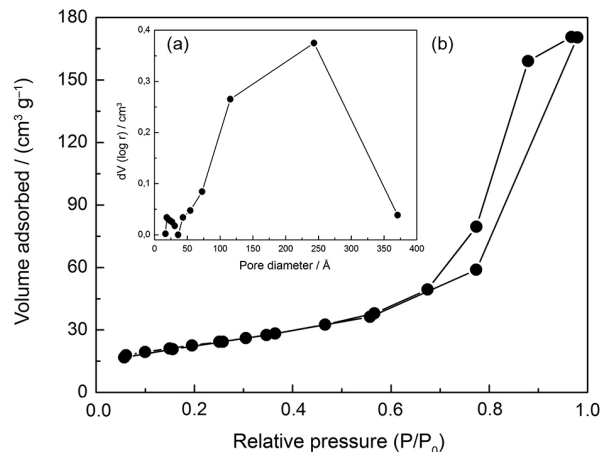

Figure 2. The pore size distribution curve obtained from the N$_2$ desorption isotherms (Barrett-Joyner-Halenda (BJH) method) (a) and N$_2$ adsorption-desorption isotherms for the catalyst (b).

The low specific surface area values obtained for the WO$_3$ crystal system can be explained based on the X-ray diffraction patterns, which indicate a characteristic monoclinic crystal system material with low surface area.
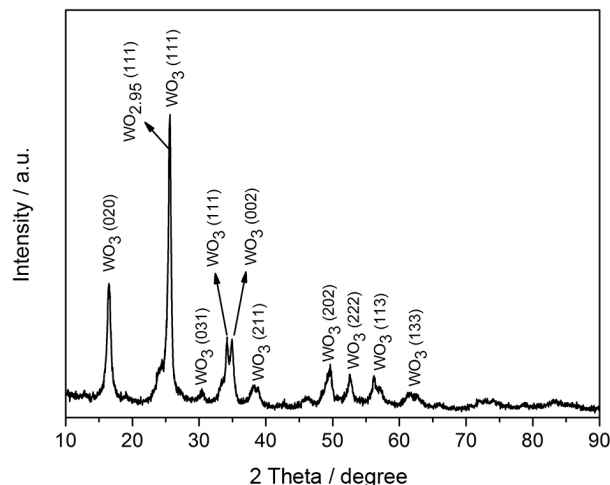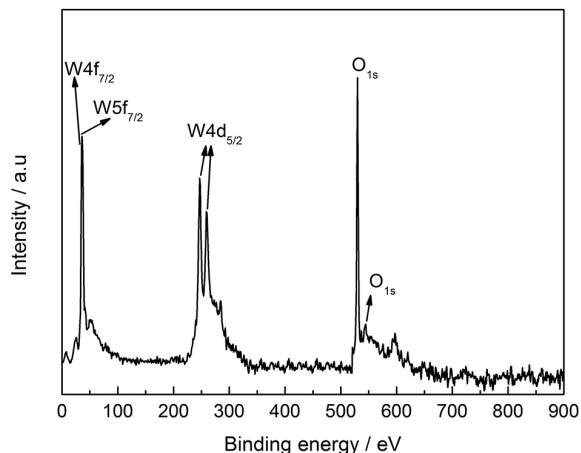

Figure 3. XRD patterns for the WO$_3$ catalyst.

The XPS analysis (Figure 4) yielded the values for the bond energy of the O$_{1s}$ electrons (529.9, 530.4 and 531.4 eV), which were attributed to three types of oxygen species: the lattice oxygen in WO$_3$, the chemically adsorbed oxygen (O^{2-}) in WO$_3$ and oxygen associated with the hydroxide (OH^{1-}).[18]

The W4f and W5f regions can be resolved by two doublets with binding energy values of W4f$_{7/2}$ (34.5 eV), W5f$_{7/2}$ (36.8 eV) and W4d$_{5/2}$ (251 and 263 eV), which can be assigned to W^{6+}, W^{5+} and W^{4+} species, respectively (W^{6+} species > W^{5+} species > W^{4+} species), before and after the catalytic reaction. All of the W surface atoms were in the highest oxidation state in the form of crystalline WO$_3$.[16,19]

Figure 5 shows the morphology of the WO$_3$ catalyst, comprised of a homogenous material with many pores, which can be favorable for catalytic oxidation. The EDX analysis confirmed the presence of the element W.

Figure 6a shows the TEM image of the WO$_3$ catalyst. A Gaussian particle size distribution was observed for tungsten,

Table 1. Textural data for the tungsten catalyst before and after calcination

Catalyst	S$_s$ / (m^2 g^{-1})	Vp / (cm^3 g^{-1})	Dp / nm	Average W size / nm[a]	Average (Scherrer) WO$_3$ size / nm[b]	W dispersion / %[c]	OSC / (mmol m^{-2})
WO$_3$ before calcination	9.54	0.032	12.87	–	–	–	7.24
WO$_3$ after calcination	7.56	0.023	11.57	109.11	58	0.12	9.48

[a]Obtained by high resolution (HR) TEM; [b]determined by XRD; [c]calculated using the formula (Wu *et al.*[17]) D$_W$ = 6n_s M$_W$ / ρ$_w$ N$_A$ d$_w$, where n_s is the number of W atoms at the surface *per* unit area (1.35×10^{19} m^{-2}), M$_W$ is the molar mass of tungsten (183.84 g mol^{-1}), ρ$_w$ is the density of tungsten (19.3 g cm^{-3}); N_A is Avogadro's number (6.023×10^{23} mol^{-1}) and d$_w$ is the average W particle size (obtained by HRTEM). S_s: specific surface area; Vp: pore volume; Dp: pore diameter; OSC: oxygen storage capacity.

Figure 4. XPS spectra for the WO₃ catalyst.

as represented in Figure 6b, and the particle size distributions for the catalysts before and after calcinations are shown in Table 1. In Figures 6c and 6d tungsten particles with a hemispherical shape at the perimeter can be observed. This result indicates only the presence of WO_3 in the catalyst, as was expected for the oxidation reaction to occur.

The results obtained from the oxygen chemisorption measurements are shown in Table 1. The oxygen storage capacity (OSC) for each sample was calculated based on the oxygen uptake. These values allow us to estimate the total amount of oxygen available in the oxide catalyst. The tungsten oxide sample presented a high OSC, indicating that this sample has a high amount of oxygen vacancies. The creation of oxygen vacancies enhanced the oxygen mobility in the tungsten oxide, as also indicated by the characterization results discussed above favoring high catalytic activity.

Catalyst performance in BTX oxidation

Figure 7 shows the conversion of BTX as a function of the reaction temperature for the catalyst studied. According to the results shown in Figure 7, it was observed that the

activity of the WO_3 catalyst increases in the order *m*-xylene < *p*-xylene < toluene < benzene.

The results obtained in the catalyst characterization suggest that the high catalytic activity observed for the WO_3 catalyst can be attributed to the presence of monoclinic WO_3, as verified by the infrared and X-ray analyses. Another possible contributing factor is a strong metal interaction, which could originate from the small lattice parameter difference between the (111), (020) and (002) lattice planes. The XPS analysis revealed the presence of three species of tungsten oxide with different oxidation states. The W^{4+}, W^{5+} and W^{6+} species present on the surface of the catalyst could react with active oxygen species favoring the oxidation process. Thus, the tungsten catalyst may increase the amount of oxygen vacancies and, in turn, the oxygen mobility and the catalytic activity. These vacancies are filled by the oxygen atoms that diffuse from the bulk to the surface of the catalyst, suggesting that the presence of crystalline defects enhances the mobility of the oxygen species.[20-22]

Another factor to be considered is the mobility of the oxygen atoms present, which are able to oxidize the hydrocarbons under study. It has been reported that the presence of oxygen vacancies is an important factor influencing the activity of some catalysts and favoring the oxidation process. An increase in the amount of oxygen vacancies can enhance the bulk and surface oxygen mobility, which appears to play an important role in oxidation reactions. The higher oxygen mobility facilitates the oxygen species migration across the catalyst structure, resulting in greater oxidation activity. It has been shown that the reduction in tungsten oxide ($W^{6+}/W^{5+}/W^{4+}$) is not due to a direct release of oxygen into the gas phase, but rather to the interaction which occurs between the surface of the catalyst and the hydrocarbon. These reactions are driven by an increased capacity for the spontaneous release of oxygen from the WO_3 system, even in the absence of a reducing agent. In the presence of the WO_3 species, the catalyst promotes the
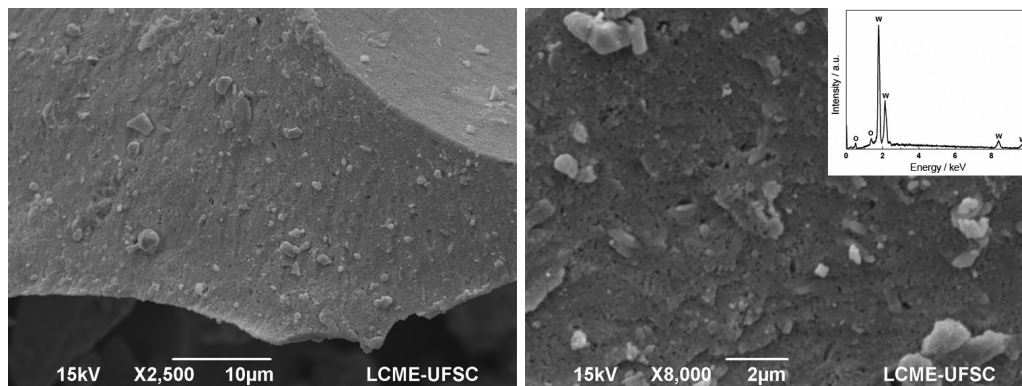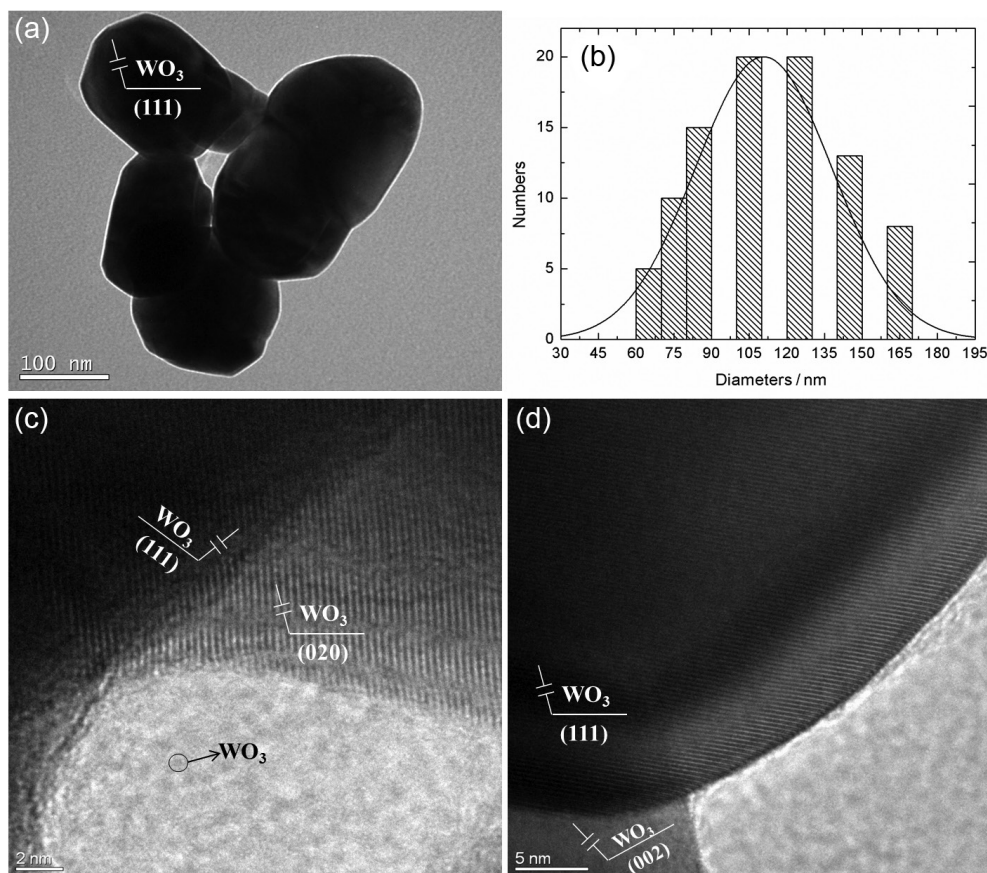

Figure 5. SEM images and EDX results for WO₃.

Figure 6. TEM image of WO₃ (a); tungsten particle size distribution (b); and HRTEM images (c and d).

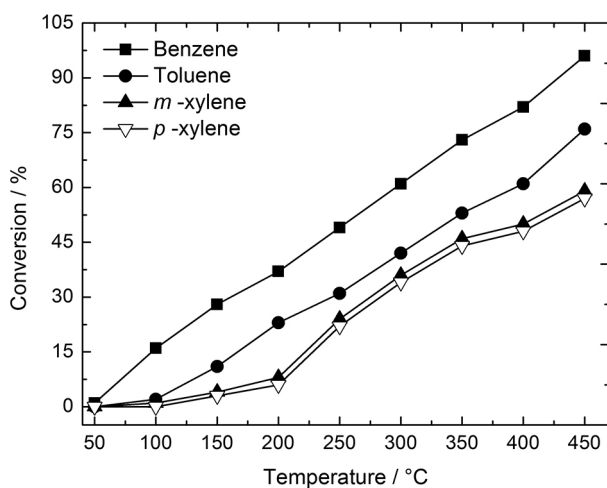**Figure 7.** BTX conversion as a function of the reaction temperature.

reduction of $W^{6+}/W^{5+}/W^{4+}$, this factor being favorable for the oxidation of hydrocarbons. These characteristics were verified by the XRD, XPS and TEM results.

The results obtained suggest that the catalytic activity of aromatic compounds is dependent on several factors, including: the strength of the carbon-hydrogen bond in the structure; the relative strength of the adsorption of each compound in question; and the ionization potential of these compounds as well as the methyl derivatives (benzene (9.24 eV), toluene (8.82 eV), *meta*-xylene and *ortho*-xylene (8.56 eV) and *para*-xylene (8.44 eV)).[17,23,24] The dependence on the ionization potential of the compounds is more evident when comparing the results obtained for *m*-xylene and *p*-xylene. In the case of *m*-xylene there was a slight decrease in the degree of conversion and this can be explained by the lower ionization potential of the compound.

Comparing the catalytic activity of the WO₃ catalyst with that of the Cu/SiO₂ catalysts described in the literature which are highly active in BTX oxidation, it can be seen that temperature $T_{benzene50}$ (benzene conversion up to 50%) is 250 °C for WO₃ and 162 °C for $SiO_{2(0.97)}Cu_{0.03}$ (described in the literature).[2] In previously published studies we use a catalyst of high surface area, which may have favored catalytic activity, while in this study we used a catalyst with a low surface area, suggesting that the catalytic activity is favored by the oxygen storage capacity on the surface, this being very favorable for catalytic oxidation reactions. Tungsten oxide has a high oxygen storage capacity favoring catalytic oxidation reactions.[2]

The catalytic oxidation of aromatic compounds involves three main steps: (*i*) the supply of oxygen by the reducible

oxide; (*ii*) the introduction of the oxygen (originating from the oxide lattice) into the substrate; and (*iii*) re-oxidation of the solid reduced by the oxygen-containing gaseous phase, which is the rate-determining step of the reaction. These steps are explained by the Mars-van Krevelen reaction mechanism.[17,25,26]

According to this mechanism, the catalytic cycle involves chemisorption of the compound (BTX) onto the WO_3 particles, in which the BTX compound migrates chemically on the surface of the WO_3. The oxygen present in the WO_3 vacancies is activated forming the active oxygen species on WO_3 and at its interfaces, the oxidation reaction then occurring between the compound and the active oxygen species. According to the Mars-van Krevelen mechanism, the BTX oxidation rate is determined by the concentration of BTX chemisorbed onto the metal oxide particles.[17,27-29]

Conclusions

The WO_3 catalyst exhibited high catalytic activity in the oxidation of benzene, toluene, and xylenes (BTX). The benzene conversion in the presence of the WO_3 catalyst exceeded 70% and the toluene conversion exceeded 50% at 350 °C. The results obtained for the studies with *meta*- and *para*-xylene suggest that the conversion of volatile aromatic compounds is also dependent on the ionization potential. The performance of the WO_3 catalyst may be due to a combination of several factors, including number of exposed active sites of tungsten oxide and greater oxygen mobility. Thus, it was verified that the catalyst based on WO_3 described herein is efficient in the conversion of BTX compounds.

Acknowledgments

References

1. Lin, C. L.; Cheng, Y. H.; Liu, Z. S.; Chen, J. Y.; *J. Porous Mater.* **2013**, *20*, 883.

2. Balzer, R.; Drago, V.; Schreiner, W. H.; Probst, L. F. D.; *J. Braz. Chem. Soc.* **2013**, *24*, 1592.

3. Alvarez-Merino, M. A.; Ribeiro, M. F.; Silva, J. M.; Carrasco-Marin, F.; Maldonado-Hodar, F. J.; *Environ. Sci. Technol.* **2004**, *38*, 4664.

4. Wang, Z.; Shen, G. L.; Li, J. Q.; Liu, H. D.; Wang, Q.; Chen, Y. F.; *Appl. Catal., B* **2013**, *138*, 253.

5. Araujo, V. D.; de Lima, M. M.; Cantarero, A.; Bernardi, M. I. B.; Bellido, J. D. A.; Assaf, E. M.; Balzer, R.; Probst, L. F. D.; Fajardo, H. V.; *Mater. Chem. Phys.* **2013**, *142*, 677.

6. Yan, Z. X.; Wei, W.; Xie, J. M.; Meng, S. C.; Lu, X.; Zhu, J. J.; *J. Power Sources* **2013**, *222*, 218.

7. Tuna, P.; Brandin, J.; *Fuel* **2013**, *105*, 331.

8. Wu, X. D.; Yu, W. C.; Si, Z. C.; Weng, D.; *Front. Environ. Sci. Eng.* **2013**, *7*, 420.

9. Feng, L.; Urnezius, E.; Luck, R. L.; *J. Organomet. Chem.* **2008**, *693*, 1564.

10. Barbosa, J.; Almeida, B.; Pereira, A. M.; Araujo, J. P.; Gomes, I.; Mendes, J.; *J. Non-Cryst. Solids* **2008**, *354*, 5250.

11. Barbosa, G. N.; Bolsoni, A. T.; Oliveira, H. P.; *J. Non-Cryst. Solids* **2008**, *354*, 3548.

12. Everaert, K.; Baeyens, J.; *J. Hazard. Mater.* **2004**, *109*, 113.

13. Alvarez-Merino, M. A.; Carrasco-Marin, F.; Moreno-Castilla, C.; *J. Catal.* **2000**, *192*, 374.

14. Alvarez-Merino, M. A.; Carrasco-Marin, F.; Fierro, J. L. G.; Moreno-Castilla, C.; *J. Catal.* **2000**, *192*, 363.

15. He, G. H.; Liang, C. J.; Ou, Y. D.; Liu, D. N.; Fang, Y. P.; Xu, Y. H.; *Mater. Res. Bull.* **2013**, *48*, 2244.

16. Signoretto, M.; Ghedini, E.; Menegazzo, F.; Cerrato, G.; Crocella, V.; Bianchi, C. L.; *Microporous Mesoporous Mater.* **2013**, *165*, 134.

17. Wu, H. J.; Wang, L. D.; Zhang, J. Q.; Shen, Z. Y.; Zhao, J. H.; *Catal. Commun.* **2011**, *12*, 859.

18. Zhang, Y. D.; He, W. W.; Zhao, H. X.; Li, P. J.; *Vacuum* **2013**, *95*, 30.

19. Di Gregorio, F.; Keller, V.; *J. Catal.* **2004**, *225*, 45.

20. Sun, G. B.; Hidajat, K.; Wu, X. S.; Kawi, S.; *Appl. Catal., B* **2008**, *81*, 303.

21. Todorova, S.; Kadinov, G.; Tenchev, K.; Caballero, A.; Holgado, J. P.; Pereniguez, R.; *Catal. Lett.* **2009**, *129*, 149.

22. Todorova, S.; Naydenov, A.; Kolev, H.; Holgado, J. P.; Ivanov, G.; Kadinov, G.; Caballero, A.; *Appl. Catal., A* **2012**, *413*, 43.

23. Naskar, S.; Naskar, S.; Mayer-Figge, H.; Sheldrick, W. S.; Corbella, M.; Tercero, J.; Chattopadhyay, S. K.; *Polyhedron* **2012**, *35*, 77.

24. Wang, Q. G.; Madix, R. J.; *Surf. Sci.* **2001**, *474*, L213.

25. Putna, E. S.; Bunluesin, T.; Fan, X. L.; Gorte, R. J.; Vohs, J. M.; Lakis, R. E.; Egami, T.; *Catal. Today* **1999**, *50*, 343.

26. Radic, N.; Grbic, B.; Terlecki-Baricevic, A.; *Appl. Catal., B* **2004**, *50*, 153.

27. Kim, Y. T.; Park, E. D.; Lee, H. C.; Lee, D.; Lee, K. H.; *Appl. Catal., B* **2009**, *90*, 45.

28. Kim, S. C.; *J. Hazard. Mater.* **2002**, *91*, 285.

29. Kim, S. C.; Shim, W. G.; *Appl. Catal., B* **2010**, *98*, 180.